

## Structural Elucidation of Immunomodulators, Acetylated Heteroglycan and Galactosamine, Isolated from *Aloe arborescens* Leaves

Jilan A. Nazeam,<sup>1</sup> Hala M. El-Hefnawy,<sup>2</sup> and Abdel-Naser B. Singab<sup>3</sup>

<sup>1</sup>Pharmacognosy Department, Faculty of Pharmacy, October 6th University, Cairo, Egypt.

<sup>2</sup>Pharmacognosy Department, Faculty of Pharmacy, Cairo University, Cairo, Egypt.

<sup>3</sup>Pharmacognosy Department, Faculty of Pharmacy, Ain Shams University, Cairo, Egypt.

**ABSTRACT** Plant polysaccharides gained extended scientific attention for their immunomodulatory effect. However, few scientific studies structurally defined polysaccharides in relation to their biological modifier response. Therefore, the study explored the effect of structurally identified isolated macromolecules from *Aloe arborescens* against cytokine modulation (interferon [IFN- $\gamma$ ], interleukins [IL-2 and IL-12], and tumor necrosis factor [TNF- $\alpha$ ]) *in vitro*. The structures were elucidated by GC, GPC, FT-IR spectroscopy, 1D NMR, COSY, HMBC, and HSQC. Two acetylated glucomannans (AANP4 and AAAP6), one deoxy-gluco galactan (AANP5), and one deoxy-N-acetyl-[1–4]-galactosamine (AANP2) were isolated. The results showed significant induction for all cytokines and the most potent component was AAAP6; acetylated phenolic glucomannan with a (1  $\rightarrow$  3)-linked glucose–mannose and (1  $\rightarrow$  4)-linked mannose backbone, which stimulated IL-12 by more than 10-fold compared with phytohemagglutinin (positive control). In conclusion, *A. arborescens* polysaccharides could be a landmark for development of effective immunotherapeutics against cancer and chronic inflammatory conditions.

**KEYWORDS:** • *Aloe arborescens* • cytokines • gluco galactan galactosamine • glucomannan • immunomodulator • structural elucidation

CANCER INCIDENCE WORLDWIDE is rising every day and cure is urgently needed. However, the currently used chemotherapy causes serious side effects. Fortunately, several previous reports have shown that some nontoxic biological macromolecules, including polysaccharides, act as immunotherapy in case of cancer disease or can increase the efficacy of conventional chemotherapy drugs.<sup>1</sup> From a pharmacological perspective, these polysaccharides are classified as biological response modifiers with the ability of enhancing cytokines, T cells, and antigen-presenting cells such as monocytes and macrophages.<sup>2–4</sup> According to Bohn and BeMiller, the most common bioactive structure building unit consists of (1–3)-linked  $\beta$ -D-glucopyranosyl units along which are randomly dispersed single units attached by 1-6 linkages.<sup>5,6</sup> Glucans, mannans, and pectic polysaccharides are the most studied immunostimulatory polysaccharides. The study focused on discovering new immunomodulatory plant polysaccharides that could be a landmark for development of effective immunotherapeutics. *In vitro* assays with structurally well-defined polysaccharides are investigated.

Polysaccharide fractions of the *Aloe arborescens* plant; water soluble polysaccharides (WAP) and alkaline soluble polysaccharides (ALP) were prepared following the protocol described previously in our study. Purity and molecular weight were determined using high-performance gel permeation chromatography (HGPC). The total polysaccharide content was estimated using a phenol–sulfuric acid spectrophotometric method. Total sugar, uronic acid, Fourier-transform infrared (FT-IR) analysis, and linkage type of bioactive polysaccharides were investigated.<sup>7</sup>

For isolation of most bioactive components, WAP and ALP were fractionated using a Diaion column (5  $\times$  20 cm, 300 g) and H<sub>2</sub>O: MeOH in a gradient manner, and the subfractions with high carbohydrate content were detected by a spectrophotometer at 490 nm.<sup>8,9</sup> WAP subfraction 4 (98.7 mg) was further chromatographed over descending paper chromatography using distilled water. Four major carbohydrate spots registered a difference in the retention factor ( $R_f$ ); (0.32, 0.61, 0.74, and 0.80). After further purification over preparative paper using butanol: acetic acid: water (BAW) (3:1:6, v/v), three components were isolated; AANP-2 (19.6 mg), AANP-4 (43.8 mg), and AANP5 (15.7 mg). The ALP fraction was further chromatographed over a Sepharose column (2  $\times$  20 cm, 50 g) using gradient NaCl solutions (0.2, 0.6, and 1.0M) that yielded the main component AAAP6 (40.1 mg).

Human peripheral blood mononuclear cells were purified from anticoagulated blood by discontinuous density

Manuscript received 6 October 2019. Revision accepted 16 November 2019.

Address correspondence to: Jilan A. Nazeam, PhD, Pharmacognosy Department, Faculty of Pharmacy, October 6th University, Cairo 12511, Egypt, E-mail: jilannazeam@o6u.edu.eg

gradient centrifugation with Ficoll-Paque to assess the immunomodulatory effect of isolated polysaccharide components through stimulation of cytokines—interferon ( $\text{IFN-}\gamma$ ), interleukins (IL-2 and IL-12), and tumor necrosis factor ( $\text{TNF-}\alpha$ )—by using ELISA kits with following manufacturer-provided protocols. Statistical analyses and significance ( $P$  values  $<.05$ ) were measured by one-way analysis of variance (ANOVA), performed using GraphPad, version 5.0. For structurally defined isolated polysaccharides, the homogeneity and molecular weights of the isolated bioactive polysaccharides were determined by high performance gel permeation chromatography.<sup>10</sup> A complete assignment by FT-IR spectrum analysis and 1D and 2D NMR methods were used to identify the isolated components.

Cytokines are messengers that allow the immune system cells to communicate to create a synchronized robust response to a target antigen. In a great effort to develop cancer treatments, many studies to characterize cytokines and exploit their vast signaling networks were done.<sup>11</sup> The results show that all cytokines ( $\text{IFN-}\gamma$ , IL-2, IL-12, and  $\text{TNF-}\alpha$ ) were significantly elevated when treated with the isolated components. Abundant release of IL-2 and IL-12 was detected, except in AANP-2 that had no effect on IL-12 production. On the other hand, AAAP6 resulted in potent modulation of IL-12 by about 10-fold of phytohaemagglu-

tin (PHA) effect (Fig. 1). The current finding approves the renewed interest in the use of polysaccharides to modulate cytokines; IL-2 and IL-12.

Chromatographic and spectroscopic investigations showed that the molecular weight of AANP2 was  $440 \text{ g mol}^{-1}$ . Molecular weight values of  $\sim 1\text{--}2 \text{ kDa}$  were detected for AANP4, AANP5, and AAAP6, as determined by HGPC data. The FT-IR spectrum revealed a typical, major, broad stretching peak of OH groups at  $3500 \text{ cm}^{-1}$  and at  $2980$  and  $1600 \text{ cm}^{-1}$  for CH stretching and C=O groups. The bands at  $890$ ,  $864$ ,  $900$ , and  $890$  and  $915 \text{ cm}^{-1}$  for AANP2, AANP4, AANP5, and AAAP6, respectively, were ascribed to  $\beta$ -configuration in galactose, glucose, and mannose of a predicted monosaccharide type.<sup>12</sup> FT-IR showed the presence of the  $\beta$ -D-glycoside linkage (1, 4-linked glucose residues), showing that the backbone comprises the 1, 4-linked Glcp. Moreover, the FT-IR absorption band indicates the presence of the acetyl ester group. In contrast, ALP spectra recorded that a characteristic band of carboxyl groups was most pronounced in the FT-IR spectrum along with other different bands of  $\alpha$ -D-linkage in galactose and mannose sugar residues (Table 1). The structures were elucidated and identified by  $^1\text{H}$  NMR,  $^{13}\text{C}$  NMR (Table 2), COSY, HMBC, and HSQC spectroscopy (Fig. 2).

Two acetylated glucomannans (AANP4 and AAAP6) were identified as different functional groups, where AANP4

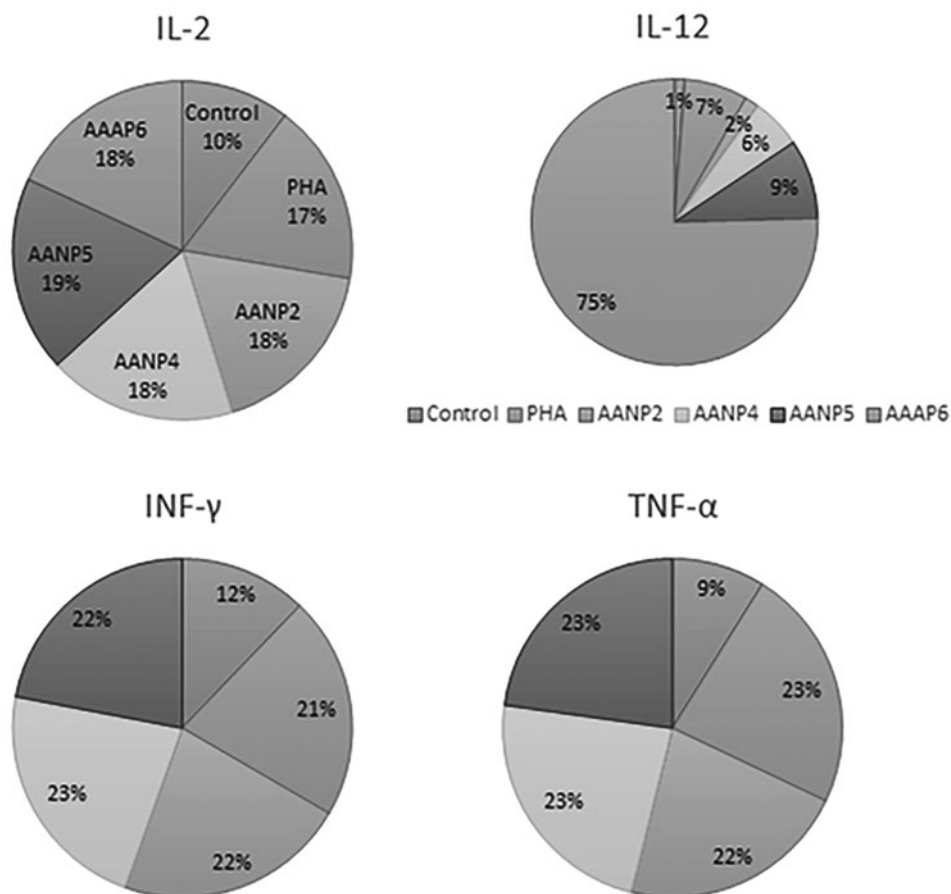


**FIG. 1.** Cytokine ELISA modulation (IL-2, IL-12, TNF- $\alpha$ , and INF- $\gamma$ ) of isolated polysaccharide components. Data are represented as mean  $\pm$  SD  $n=3$ . Statistical analyses were carried out using one-way ANOVA, followed by the Tukey *post hoc* test. ANOVA, analysis of variance; ELISA, enzyme-linked immunosorbent assay; IL-2, interleukin-2; SD, standard deviation; TNF- $\alpha$ , tumor necrosis factor- $\alpha$ .

TABLE 1. WEIGHT-AVERAGE MOLECULAR WEIGHTS (Mw, G MOL<sup>-1</sup>), NUMBER-AVERAGE MOLECULAR WEIGHTS (Mn), POLYDISPERSITY (Mw/Mn), AND CHARACTERISTIC FOURIER-TRANSFORM INFRARED SIGNALS OF ISOLATED COMPONENTS

Isolated components	Mw	Mn	D (Mw/Mn)	IR region (cm <sup>-1</sup> )	Anomeric configuration/monosaccharide type
AANP2	4.4 × 10 <sup>2</sup>	1.6 × 10 <sup>2</sup>	2.7 × 10 <sup>0</sup>	890	β-D-Galactose/β-D-Glucose/β-D-Mannose
AANP4	1.9 × 10 <sup>3</sup>	4.0 × 10 <sup>2</sup>	4.7 × 10 <sup>0</sup>	864	β-D-Galactose
AANP5	1.9 × 10 <sup>3</sup>	1.7 × 10 <sup>2</sup>	1.1 × 10 <sup>1</sup>	900	β-D-Galactose/β-D-Glucose
AAAP6	2.0 × 10 <sup>3</sup>	3.6 × 10 <sup>2</sup>	5.6 × 10 <sup>0</sup>	890 915	β-D-Galactose/β-D-Glucose/β-D-mannose β-D-Galactose

Mw, molecular weight.

components contain the deoxy group and AAAP6 components carry a phenolic cycle. The <sup>13</sup>C NMR spectrum of AANP4 was found to match that of glucomannan, and the relevant functional groups were confirmed by FT-IR. In addition, the large *J* value of protons in the sugar residue (*J* = 7 Hz) indicated the presence of axial to axial coupling, suggesting that mannan was a backbone unit of the sugar moiety. In the <sup>1</sup>H NMR spectrum, three characteristic peaks appeared downfield at 1.1 ppm (triplet), 1.2 ppm (doublet), and 1.3 ppm (doublet), indicating the presence of three different alkyl groups in different chemical environments. 2D-NMR: The COSY spectrum showed three anomeric proton signals at δ 4.69, 4.71, and 4.74 ppm (*J* = 8, 12 Hz), which confirmed a β-glycosidic linkage. This result supported the agreement with IR spectral data. The sharp high-intensity signal at 2.2 ppm was assigned to the acetyl group in residue C. Two doublet symmetrical signals at 2.8 and 3.0 ppm were attributed to H-6 in residues A and C, the C6 presumably shielded by a carboxylic group (downfield signals at δ 177.4 and 180.6 ppm), respectively. Moreover, the deshielded signals at 5.2 and 5.5 ppm were assigned to alkene protons in residue B.

**Residue A (assigned to β-D-4-deoxy-mannouronic-p);** in the HMBC (<sup>1</sup>H, <sup>13</sup>C) spectrum, signals were observed for a methyl proton at C-4 at δ 1.3 ppm, which associated with a cross peak between C-2 at δ 68.0 ppm and an acidic car-

bonyl carbon at δ 182.5 ppm, thus confirming its location at C-4. As a consequence, the H-4 signal at 2.2 ppm formed a cross peak with a signal at 30.2 ppm, which was assigned to C-6. In the <sup>13</sup>C NMR spectrum, the C-4 signal in residue A appeared upfield at 30.31 ppm because of the methyl proton substitution expected at this position according to the (<sup>1</sup>H-<sup>13</sup>C) correlation in HMBC.

**In residue B (β-D-6-deoxy-3-acetylated-Glup),** the proton signals of the alkene chain (HC<sub>b</sub> = 6.1 ppm) formed a cross peak with δ 18.3 (CH<sub>3</sub>) at 70.0 ppm (C-2). These spectral data indicated the presence of a terminal methyl group on the trans-alkene chain. Furthermore, another cross peak was detected at 139.2 ppm and attributed to the other olefinic group. This olefinic proton signal also formed a cross peak with the signal at 3.6 ppm, which was ascribed to H-5. Therefore, the alkene chain was expected to be located at C-3. The downfield C-5 signal at δ 56.9 ppm showed a cross peak with a methyl signal at 1.1 ppm, which was assigned to C-6. Additionally, the anomeric proton signal at 103.1 ppm correlated with the signal at 3.6 ppm, which was assigned to H-5. The COSY showed three sets of interactions of directly coupled protons: pairs of proton signals at 4.1 ppm and 1.3 ppm and at 3.7 ppm and 4.7 ppm were assigned to (H-4/CH<sub>3</sub>) and (H-2/H-1) in residue A, and proton signals at 3.6 ppm and 1.2 ppm were attributed to (H-5/CH<sub>3</sub>) in residue B.

TABLE 2. C<sup>13</sup> NMR ASSIGNMENT OF AANP-2, AANP-4, AND AAAP-5 MONOSACCHARIDE RESIDUES (δ, PPM)

Carbons	AANP2 Residues		AANP4 Residues			AANP5 Residues		
	A β-D-acetylated -GalNHp	B α-D-deoxy- GalNHp	A β-D-4-deoxy- mannouronic-p	B β-D-6-deoxy-3- acetylated-Glup	C β-D-2-acetylated -mannouronic-p	A β-D-6- deoxy-galp	B α-D- Glup	C β-D-6- methoxy-galp
C-1	101.15	99.20	99.67	104.45	99.67	96.22	104.06	114.07
C-2	72.92	57.12	72.38	71.92	73.01	71.12	70.43	73.12
C-3	69.04	69.04	85.87	78.06	68.94	74.05	78.13	74.05
C-4	76.07	89.29	30.31	77.45	77.45	75.06	80.37	75.06
C-5	71.64	72.98	74.61	56.91	73.30	74.05	72.51	76.67
C-6	37.03	37.03	30.31	20.21	30.31	29.51	60.97	69.97
CH <sub>3</sub>	—	16.92	16.68	11.01	20.23	14.54	—	—
C=O	—	—	177.27	—	164.03–180.60	—	—	—
CH <sub>2</sub>	—	—	—	30.7	—	—	—	—
CH (a,b)	—	—	—	138.59 (a), 104.48 (b)	—	—	—	—
CH <sub>3</sub> -AC	31.93	—	—	—	—	—	—	—
OCH <sub>3</sub>	53.03	52.12	—	—	—	—	—	52.77
NH-C=O	165.03	165.03	—	—	—	—	—	—
CH <sub>3</sub> -C=O	164.72	—	—	—	—	—	—	—

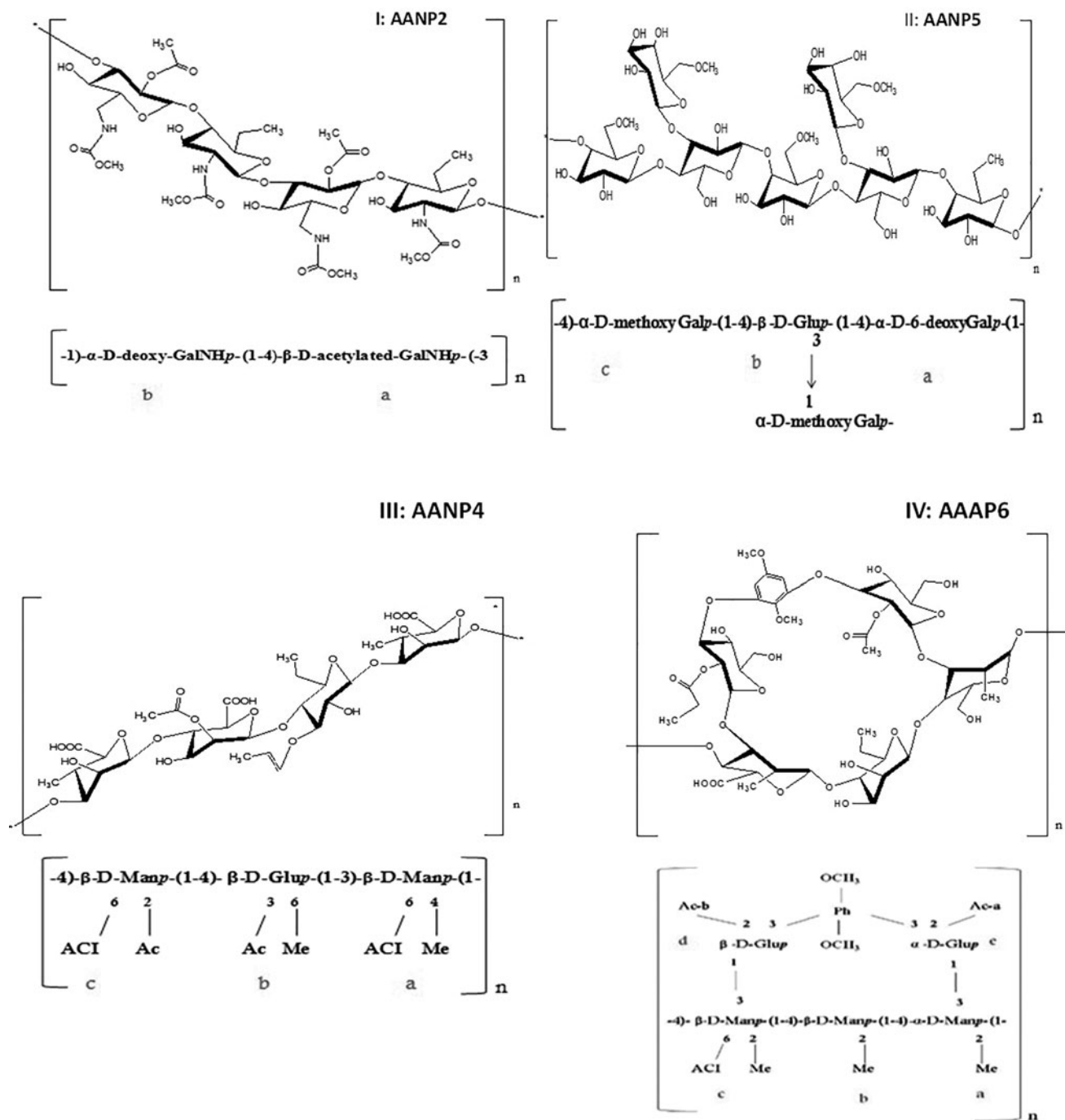


**FIG. 2.** Supposed structures of isolated components of the water-soluble fraction (WAP); AANP2, AANP4, AANP5 and the alkali-soluble fraction (ALP); AAAP6. ALP, alkaline soluble polysaccharides; WAP, water soluble polysaccharides.

*In residue C ( $\beta$ -D-2-acetylated mannuronic-p),* the anomeric proton signal at 4.7 ppm showed a cross correlation with two different types of carbonyl carbon signals: one at 170.0 ppm (acetylated carbonyl) and one at 192.2 ppm (acidified carbonyl), suggesting the presence of a 2-acetyl, 6-uronic acid moiety. Additionally, the C-3 of residue A and C-4 of residues B and C appeared downfield at 85.87 and 77.45 ppm as a result of the expected (1-3) and (1-4) link-

ages. The C-6 signal appears at 30.0 ppm for residues A and C because of carboxylic group substitution. On the other hand, the methyl group at C-6 of residue B shifted the signal downfield to 20.2 ppm. C-3 in residue B and C-2 in residue C were deshielded by  $\text{OC}_3\text{H}_5$  and  $\text{OCOCH}_3$  groups and assigned to the peaks at 78.0 and 73.01 ppm, respectively. The structure of AANP4 was determined to be related to that of deoxyacetylated glucomannan.

AAAP6 components (acetylated phenolic glucomannan): From the FT-IR spectral data, the supposed sugar moiety is a glucomannan. These data were in accordance with a previously published study on characterization of polysaccharides from *A. arborescense*.<sup>13</sup> **1D-NMR; From <sup>1</sup>H-NMR**, three characteristic peaks at  $\delta$  1.18 (triplet), 1.34 (doublet), and 1.47 (doublet) ppm indicate the presence of deoxy sugar at a different position of the moiety. The peak of acetylation was identified at 2.25 ppm, while the peak at 2.75 ppm was attributed to H-6 at residue B. The high, integrated singlet peak at 3.36 ppm is expected to be related to methoxy groups. Moreover, the quartet signal at 3.66 ppm is assigned to acetylated alkene substitution in residue D. The triplet signal at 3.67 ppm is attributed to substituted H-2 (by acetyl group) in residues d and e. Furthermore, the peak detected at 7.1 ppm indicated the probability of phenolic moiety presence in the structure.

**2D-NMR; From the COSY spectrum**, geminal correlation was observed between alkene protons (acetylated) (at  $\delta$  3.6 ppm) and methyl protons ( $\delta$  1.1 ppm) in supposed residue d. Five anomeric protons were observed at 4.7, 4.8, 4.9, 5.1, and 5.2 ppm, referring to the presence of three  $\beta$ -glycosylation and two  $\alpha$ -glycosylation linkage types. **From the HSQC spectrum**, the correlation at 3.4/20, 3.6/60.1, 3.1/40, 5.4/80, and 3.5/53.5 ppm was assigned to CH<sub>3</sub> of acetyl, H-6/C-6 (residue E), H-6/C-6 (residue C), H-2/C-2 (residue d), and the methoxy group, respectively. **From the HMBC (<sup>1</sup>H, <sup>13</sup>C) spectrum, residue a ( $\alpha$ -D-2-deoxy-Manp-)**, the cross peak at 4.0/55 ppm was assigned to (H-5/C-2), which refers to the presence of the methyl group at this position. Moreover, the anomeric proton at 95.3 ppm showed a correlation with 4.3 ppm attributed to H-3. **Residue b ( $\beta$ -D-6-deoxy-Manp-)**; the methyl substitution at 10.2 ppm showed a cross peak with 3.6 ppm elucidated by H-4, while the 3.9/20 ppm cross peak is supposed to be related to (H-5/C-6) correlation.

**Residue c ( $\beta$ -D-2-deoxy-Man-uronic-p-)**; carbonyl of carboxylic substitution (182.5 ppm) showed a correlation with downfield H-3 at 4.4 ppm (3-linkage type). The upfield signal at 65.3 ppm assigned to C-5 formed a cross peak with H-4 at 4.0 ppm (4-linkage type). **Residue d ( $\beta$ -D-2-Ac-3-Ph-Glup-)**; the linkage (1-3) between residues C and D was identified by a cross peak at 4.7/105.2, 80.1 ppm, which is assigned to H-1 of residue C/C-1 of residue D, and C-2 in consequence. H-3 at 4.2 ppm (deshielded) formed two cross peaks; the first one with C-2 at 80.1 ppm (this attribution indicates that the acetyl substitution is located at this position). The second peak with 56.3 ppm is ascribed to the methoxy group of phenolic moiety at 56.3 ppm, which confirms the presence of methoxy at the 6-position. Additionally, the contribution of the phenolic structure as a bridge form between the sugar moieties<sup>14</sup> is also verified. This elucidation is supported by the correlation detected between methoxy in the phenolic group and H-4 at 3.5 ppm.

**Residue e ( $\alpha$ -D-2-Ac-3-Ph-Glup-)**; a strong long-range correlation (H-2/C-3-Ph) at 5.2/160.1 ppm confirmed the assignment of the phenolic bridge between residues D and E

and location of methoxy at C-3. The cross peak at 4.0/55.6 is attributed to H-3/OCH<sub>3</sub>-Ph. The carbonyl of the acetyl form at 175.4 ppm showed two cross peaks with H-3 and H-4 at 4.1 and 3.4 ppm. Linkage (1-3) glycosylation was detected (H-4=3.4/C-3=82.5 ppm) by cross peak investigation, this indicated the presence of the phenolic group at C-3 of residue E. Branched moiety of residue e at residue a was identified by a cross peak (5.1/95.5 ppm) assigned to H-3 residue A/C-1 residue E. It was worth noting that the highly deshielded proton of H-3 in residue A resulted from glycosylation at this position b and glycosylation at H-4. AAAP6 is identified as an acetylated phenolic glucomannan (Fig. 2).

**AANP2 components (deoxy-N-acetyl-[1-4]-galactosamine): 1D-NMR:** The <sup>13</sup>C NMR spectrum matched that of galactose monosaccharide, and the presence of galactose was confirmed by FT-IR. In addition, two anomeric protons at 4.7 and 5.1 ppm were detected, which was consistent with signals at 103.1 and 99.2 ppm in the <sup>13</sup>C NMR, which indicated the presence of a  $\beta$ -glycosylated residue and  $\alpha$ -glycosylated moiety. The small J coupling constant (4 Hz) in the <sup>1</sup>H NMR refers to the presence of axial to equatorial coupling. In the <sup>1</sup>H NMR spectrum, two characteristic singlets of equal integration at 2.9 and 3.1 ppm indicated the presence of two methoxy protons in different positions, which were consistent with signals at 53.03 and 52.12 ppm in the <sup>13</sup>C NMR. Moreover, the signals at 1.9 and 2.6 ppm were assigned to acetyl protons. The triplet at 1.3 ppm revealed the presence of 6-deoxyhexosyl residues, while the quartet at 3.6 ppm was attributed to the H-5 proton in the sugar region owing to the mode of splitting. This result indicated that H-4 was free from substitution, increasing the probability of the presence of a (1-3) linkage.

The aromatic signals at 7.9 and 8.1 ppm were attributed to the probable presence of two amide groups in different positions. The C-2 signal in both sugar residues appeared upfield at 57.12 ppm and refers to the proposed NH substitution at this position. The downfield proton signals of C-4 at 89.29 ppm confirmed the previous Smith degradation result, indicating a (1-4) linkage. The characteristic deshielded signal at 37.03 ppm confirmed the presence of an alkyl substitution at C-6. The signal of the methyl group of an acetate was expected at 31.9 ppm, and the corresponding carbonyl carbon signals appeared at 165.0 and 171.2 ppm, indicating the presence of two carbonyl carbons in different chemical environments (Table 2).

**Residue A (assigned as  $\beta$ -D-acetylated-GalNHp);** In the HMBC (<sup>1</sup>H, <sup>13</sup>C) spectrum, a long-range correlation was observed between the H-6 signal at  $\delta$  31.4 ppm and the NH signal at 7.9 ppm. The amide carbonyl signal at 164.7 ppm formed cross peaks with signals of H-6 and NH at 2.9 and 8.1 ppm, respectively. In addition, methyl proton signals at 16.6 ppm correlated with the H-5 signal at 3.6 ppm. The signal at 76.07 ppm was assigned to deshielded C-4 and formed a cross peak with signals of H-3 (3.00 ppm) and H-6 (2.9 ppm). **2D-NMR:** The COSY spectrum revealed two sets of interactions between coupled protons. First, a proton at 7.9 ppm that was assigned to NH was coupled with signals at

2.9 and 3.1 ppm, which represented methoxy protons. These interactions confirmed the presence of galactosamine residues. Second, the anomeric proton at 4.7 ppm was coupled with a downfield sugar proton signal at 3.5 (quartet), which was assigned to H-5 of residue A.

**In residue B (assigned as  $\alpha$ -D-Deoxy-GalNHp)**, the resonance of H-3 of residue A at 3.01 ppm formed cross peaks with signals of the methyl carbon of an acetyl group at 31.0 ppm, a carbonyl carbon at 164.7 ppm, and an anomeric carbon at 119.3 ppm. The amide proton signal at 7.9 ppm correlated with those of C-6 at 37.4 ppm and of a carbonyl carbon (amide) at 164.7 ppm. The signal of C-6 formed a cross peak with 3.5 ppm, which was assigned to H-5. Moreover, the signal of the carbonyl of an acetate group at 171.0 ppm formed a cross peak with the signal at 3.8 ppm, which was assigned to H-2. In addition, the methoxy group signal at 52.7 ppm correlated with the H-2 signal at 3.9 ppm and a signal at 3.6 ppm, which was assigned to H-4. AANP2 was thus classified as a deoxy-N-acetyl-[1-4]-galactosamine and its predicted structure is shown in Figure 2.

AANP5 components (deoxy-glucogalactan): 1D-NMR: A glucogalactan backbone moiety was postulated to be the AANP5 component. The coupling constant of sugar protons was equal to 4 Hz, indicating the presence of axial to equatorial coupling. Therefore, the sugar moiety was surmised to be galactose and/or glucose, which was in good agreement with FT-IR spectra and  $^{13}\text{C}$  NMR signals. In the  $^1\text{H}$  NMR spectrum, the region 2–3 ppm was signal free, and no carbonyl carbon was observed in the  $^{13}\text{C}$  NMR, indicating that the moiety was not acetylated. In DEPT  $^{13}\text{C}$  NMR, the secondary carbon of C-6 was detected at 60.5 ppm with a high intensity, which indicated that the OH at this carbon was free for most sugar residues. The methoxy group was identified as a singlet at 4.2 ppm in  $^1\text{H}$  NMR and  $\delta$  52.77 ppm in  $^{13}\text{C}$  NMR. 2D-NMR: In the COSY spectrum, three anomeric proton signals were detected at 4.4, 4.6, and 5.2 ppm, indicating the presence of 2  $\beta$ -glycosylations and one  $\alpha$ -glycosylation. The anomeric carbon signal at 5.2 ppm in residue B showed correlations with the H-1 and H-2 signals at 3.7 and 3.9 ppm, respectively, while the methoxy group signal at 3.7 ppm correlated with the H-6 signal at 4.1 ppm in residue C. In the HSQC spectrum, correlations at 1.0/15.6, 3.2/50.1, and 2.1/29.5 ppm were assigned to  $\text{CH}_3$ ,  $\text{OCH}_3$ , and H-6/C-6, respectively.

**Residue A (assigned to  $\beta$ -D-6-Deoxy-Galp)**; a triplet at 1.1 ppm corresponding to a signal of 14.2 ppm in  $^{13}\text{C}$  NMR was attributed to a methyl substitution at C-6. In the HMBC ( $^1\text{H}$ ,  $^{13}\text{C}$ ) spectrum, in residue A ( $\beta$ -D-2-deoxy-Galp), the H-5 peak (3.4 ppm) correlated with the upfield signal of C-6 (23.8 ppm). This result confirmed the presence of a methyl substitution at this position. The H-2 signal at 3.9 ppm formed a cross peak with the signal at 71.6 ppm, which was assigned to C-3. In addition, the anomeric carbon signal at 104.4 ppm correlated with the signal at 3.6 ppm, which was attributed to H-3.

**In residue B ( $\alpha$ -D-Glup)**, the anomeric proton signal at  $\delta$  5.1 ppm formed a cross peak with the C-2 signal at  $\delta$  78.3 ppm. The correlation at 3.1/59.1 ppm was attributed

to (H-5/C-6). The expected *O* glycosylations at C-4 and C-3 were confirmed by the cross peak at 4.4/80.3 ppm, which was assigned to (H-4/C-3). In residues B and C, C-6 was more deshielded because of methoxy substitution and was expected to appear downfield ( $\delta$  69.97 ppm) relative to C-6 in residues A and B ( $\delta$  66.1 and 60.9 ppm).

**In residue C ( $\beta$ -D-6-methoxy-Galp)**, the proton signal at 52.0 ppm, attributed to a methoxy group, showed a cross peak with the H-1 signal at 5.3 ppm. In addition, the H-2 signal at 3.5 ppm showed a correlation with the C-1 signal at 116.1 ppm, while the peak at 3.6/72.0 ppm referred to (H-4/C-3). The branched Cb residue (methoxy-Galp) was identified in light of the cross peak between the anomeric proton signal at 5.1 ppm and the anomeric carbon signal at 114.8 ppm, which were assigned to H-1 of residue B and C-1 of residue C. AANP5 was identified as deoxyglucogalactan (Fig. 2).

Structure–activity relationships are critical to various aspects of drug discovery, ranging from primary screening to lead optimization. There are many parameters that may affect the potency of components in efforts to elucidate the details through theoretical modeling of the isolated components.<sup>15</sup> The five isolated components derived from *A. arborescens* were interpreted to investigate the structure–activity relationship between polysaccharides and *in vitro* immunomodulating activity. Factors considered included molecular weight, monosaccharide unit of main chains, configuration of glycosidic bonds, degree of side-chain branching, and structural modification of functional groups.

The results show that the increase in molecular weights has no correlation with modulation of four tested cytokines. Where the AAAP6 components possess a low molecular weight, they have the highest activity against IL-2, IL-12, and TNF, respectively. It was obvious that galactose and mannose appeared critical in modulation of IL-2, TNF $\alpha$ , and INF.  $\beta$ -Configurations, branching, and acetylation seem to be important factors influencing activity in case of isolated components. Moreover, the phenolic content of AAAP6 may potentiate the effect against IL-2 by about 10-fold in comparing positive control PHA. However, the amide content probably has no tremendous effect in immunomodulation, where AANP2 did not show significant activity compared with PHA. This finding can help in the design of novel polysaccharide drugs, which has essentially been a trial-and-error process despite the efforts devoted to it by pharmaceutical research groups. This preliminary investigation could be used to develop new immunotherapy products with the aid of *in silico* computer programming. Moreover, the potential use of these unique, biological modifier components as a new vaccination strategy against cancer, chronic inflammatory conditions, autoimmunity, infectious diseases, and allergies is suggested. Further *in vivo* pharmacological evaluation is required to determine the mechanism of action.

#### AUTHOR DISCLOSURE STATEMENT

The authors have declared that no competing interests exist.

## FUNDING INFORMATION

No funding was received for this article.

## REFERENCES

1. Zong A, Cao H, Wang F: Anticancer polysaccharides from natural resources: A review of recent research. *Carbohydr Polym* 2012;90:1395–1410.
2. Tzianabos AO: Polysaccharide immunomodulators as therapeutic agents: Structural aspects and biologic function. *Clin Microbiol Rev* 2000;13:523–533.
3. Kuroki M, Miyamoto S, Morisaki T, Yotsumoto F, Shirasu N, Taniguchi Y, Soma G: Biological response modifiers used in cancer biotherapy. *Anticancer Res* 2012;32:2229–2233.
4. Leung MYK, Liu C, Koon JC, Fung KP: Polysaccharide biological response modifiers. *Immunol Lett* 2006;105:101–114.
5. John BA, Bemiller JN: (1 → 3)- $\beta$ -D-Glucans as biological response modifiers: A review of structure-functional activity relationships. *Carbohydr Polym* 1995;28:3–14.
6. Ferreira, SS, Passosa CP, Madureira P, Vilanova M, Coimbra MA: Structure–function relationships of immunostimulatory polysaccharides: A review. *Carbohydr Polym* 2015;132:378–396.
7. Nazeam JA, Gad HA, Esmat A, El-Hefnawy HM, Singab AB: *Aloe arborescens* polysaccharides: In vitro immunomodulation and potential cytotoxic activity. *J Med Food* 2017;20:491–501.
8. Masuko T, Minami A, Iwasaki N, Majima T, Nishimura S, Lee YC: Carbohydrate analysis by a phenol—Sulfuric acid method in microplate format. *Anal Biochem* 2005;339:69–72.
9. Dubois M, Gilles K, Hamilton JK, Rebers PA, Smith F: Colorimetric method for determination of sugars and related substances. *Anal Chem* 1956;28:350–356.
10. You L, Gao Q, Feng M, Yang B, Ren J, Gu L, Cui C, Zhao M: Structural characterisation of polysaccharides from *Tricholoma matsutake* and their antioxidant and antitumour activities. *Food Chem* 2013;138:2242–2249.
11. Lee S, Kim margolin: Cytokines in cancer immunotherapy. *Cancers* 2011;3:3856–3893.
12. Wiercigroch, E, Szafraniec E, Czamara K, Pacia MZ, Majzner K, Kochan K, Kaczor A, Baranska M, Malek K: Raman and infrared spectroscopy of carbohydrates: A review. *Spectrochim Acta A Mol Biomol Spectrosc* 2017;185:317–335.
13. Wozniowski T, Blaschek W, Franz G: Isolation and structure analysis of a glucomannan from the leaves of *Aloe arborescens* var. miller. *Carbohydr Res* 1990;198:387–391.
14. McManus JP, Davis KG, Beart JE, Gaffney SH, Lilley TE, Haslam E: Polyphenol Interactions. Part 1. Introduction; some observations on the reversible complexation of polyphenols with proteins and polysaccharides. *J Chem Soc Perkin Trans* 1985;2:1429–1438.
15. Qi Chang D, Miao Y, Lang L, Yu Bin J: Research on structural modification and structure-activity relationship about anti-tumor of polysaccharides from plants. In: *Applied Mechanics and Materials*. Stafa-Zurich, Switzerland: Trans Tech Publications Ltd., 2013, pp. 3232–3236.